



# Pyrolysis temperature changes the physicochemical characteristics of water hyacinth-based biochar as a potential soil amendment

Ashenafei Gezahegn<sup>1,2</sup> · Yihenew G. Selassie<sup>1</sup> · Getachew Agegnehu<sup>3</sup> · Solomon Addisu<sup>1</sup> · Fekremariam Asargew Mihretie<sup>4</sup> · Yudai Kohira<sup>5</sup> · Shinjiro Sato<sup>5</sup>

Received: 4 October 2023 / Revised: 12 January 2024 / Accepted: 16 January 2024  
© The Author(s), under exclusive licence to Springer-Verlag GmbH Germany, part of Springer Nature 2024

## Abstract

Temperature greatly determines biochar's physicochemical characteristics during the pyrolysis of a biowaste. This study aimed to investigate how pyrolysis temperature alters the physicochemical characteristics of water hyacinth (WH) biochar as a soil amendment. WH biomass was slowly pyrolyzed at three temperatures (350, 550, and 750 °C) for 2 h. Results show that biochar yield lessened from 51.0 to 33.3% with a temperature rise. When pyrolysis temperature increased biochar's pH (9.24–11.2), electrical conductivity (28.0–44.7 mS cm<sup>-1</sup>), liming capacity (17.7–33.0% CaCO<sub>3</sub> equivalence), ash content (33.3–52.4%), available nutrients (Ca, Mg, K, P), surface area (1.1–29.8 m<sup>2</sup> g<sup>-1</sup>), pore volume, C/N ratio (15.9–20.3), and water holding capacity increased. However, C, H, N, H/C (0.89–0.11) and O/C (0.62–0.49) ratios, cation exchange capacity (CEC) (44.4–2.3 cmol<sub>+</sub> kg<sup>-1</sup>), and pore width decreased. Surface functional groups shrank when pyrolysis temperature increased. As the temperature rises, WH biochar becomes structured, porous, and recalcitrant. All WH biochar samples show high alkalinity, particularly developed at 550 °C and 750 °C could replace liming materials in soil acidity alleviation. Biochar produced at 350 °C and 550 °C could improve agricultural soil fertility and nutrient retention capacity due to the lower C/N ratio, high N content, and CEC. Biochar produced at 550 °C and 750 °C can sequester carbon in the soil. Biochar developed at 750 °C be applied to amend soil physical properties due to its comparably high surface area and porosity. Hence, the thermal conversion of WH biowaste to biochar helps obtain suitable biochar properties for soil amendment.

**Keywords** Aquatic weed · Lake Tana · Waste management · Biochar · Soil fertility

## 1 Introduction

A carbon-enriched substance called biochar is frequently used as an amendment of soil to enhance the quality of soil [1]. Soil chemical, physical, and biological aspects may be improved when using biochar as an amendment for soil [2]. The effect of biochar on soil fertility is mostly due to the larger specific area, well-structured pores, high CEC, plenty of liming, and available nutrients from biochar [3]. Applying biochar to soil enhanced soil's chemical properties including pH, CEC, total N and available P [4], organic carbon [5], and base saturation [6]. Moreover, biochar promotes the enzymatic reaction and microbial biomass in soil [7], escalating the soil's capacity to supply nutrients to plants [8]. Additionally, biochar lowers the soil's bulk density [9], increases porosity [10], and thereby improves the soil's capability to retain water [11] and reduces nutrient leaching [12]. Accordingly, adding biochar to soil significantly increases soil fertility, boosts plant growth [3], and improves crop yield

✉ Ashenafei Gezahegn  
ashenafigezahegn@gmail.com

<sup>1</sup> Department of Natural Resources Management, College of Agriculture and Environmental Sciences, Bahir Dar University, Bahir Dar, Ethiopia

<sup>2</sup> Department of Natural Resources Management, College of Agriculture and Environmental Sciences, Debark University, Debark, Ethiopia

<sup>3</sup> International Crops Research Institute for Semi-Arid Tropics, Addis Ababa, Ethiopia

<sup>4</sup> Agriculture and Food, CSIRO, Black Mountain, 2-40 Clunies Ross Street, Acton ACT 2601, Australia

<sup>5</sup> Department of Science & Engineering for Sustainable Innovation, Faculty of Science and Engineering, Soka University, 1-236 Tangi-Machi, Hachioji, Tokyo 192-8577, Japan

in acid and nutrient-deficient soils [13]. However, the soil amendment qualities of biochar are partly determined by the distinct physicochemical characteristics of biochar [14].

Biochar is produced via pyrolysis, where biomass thermal degradation occurs at high temperatures in an oxygen-free environment [15]. The biomass type and pyrolysis conditions have an important effect on the physicochemical characteristics of biochar [16, 17]. Among pyrolysis conditions, temperature greatly affects several biochar physicochemical properties [18]. Studies show that as pyrolysis temperature rises, biochar pore volume, specific surface area, ash and carbon contents, and total P and Ca concentrations increase while cation exchange capacity (CEC), volatile matter, and total N decrease [17, 19]. Such changes in biochar physicochemical characteristics are greatly associated with the loss of volatiles in higher temperatures of pyrolysis [20]. Likewise, various commonly available raw materials are utilized as feedstock for biochar production, such as plant and crop residues, wood chips, animal manures, and organic wastes [21]. Over the recent few years, due to its advantages in terms of sustainability, economics, and rising demand in the sectors of energy and the environment, there has been growing attention to converting biowaste into biochar [22]. Several essential components and minerals are present in biochar made from biomass including wastes from invasive plants [23].

Water hyacinth (WH) (*Eichhornia crassipes*), known as “Emboch” in Ethiopia, native to the Amazon Basin, South America, is categorized among the hundred very harmful encroaching species and one of the world’s ten worst weeds [24]. The first incidence of WH in Ethiopia was reported in 1965 [25]. Since 2011, WH remains a major problem at Ethiopia’s largest freshwater lake, Lake Tana [26]. In 2020, 30,728 ha (10%) of the lake’s surface was covered by WH mat [27]. The weed caused several problems, particularly in the agriculture, aquaculture, shipping, hydroelectricity, and ecotourism industries [28]. To control the weed infestation, nearly a million laborers have been devoted and over US \$3.2 million has been spent. Despite this fact, the efforts made so far have not yet played a significant role [29]. The major controlling strategy, physical weed removal was proven to be ineffective because of the massive biowaste disposition issues and the weed’s quick growth [30].

Since eradicating water hyacinths is very difficult, sustainable management techniques have been suggested to reduce detrimental effects on surrounding ecological and socioeconomic structures [31]. For instance, the transformation of WH biomass into biochar can be a potential option for soil fertility improvement and carbon sequestration and in turn assists in weed disposal management [32, 33]. Being rich in hemicellulose (48%) and cellulose (20%) and its lower lignin content (3.5%), WH can be a potential biomass for producing numerous valuable products [34].

Additionally, biomass production of WH is extensive, annually producing more than a hundred tons per hectare, and also comprises crucial plant-growing elements that make the weed biomass a promising supply source for soil amendment after pyrolysis [33].

Although researches regarding the conversion of WH into biochar as a soil amendment are few, studies have been conducted on turning WH biomass for different uses including soil use, nutrient extraction, and contaminant sorption. For instance, Masto et al. [33] explored the effect of a range of pyrolysis temperatures (200–500 °C) and retention time of 30 to 120 min on WH biochar stability and the impact it had on soil biochemical characteristics and corn seedling growth. Bottezini et al. [32] also studied how pyrolysis temperature affected WH biochar chemical and molecular constituents and P forms and availability as a potential soil amendment under varying temperatures, viz. 400–600 °C. Bordoloi et al. [35] reported a beneficial impact of WH biochar on water retention ability and minimizing soil cracking. Jutakanoke et al. [36] demonstrated an enhanced role of WH biochar made at 500 °C on convolvulus growth and soil acidity amendment. Also, Zhang et al. [37] conducted a study on the influence of WH biochar prepared at a temperature range of 250–550 °C for Cd adsorption. Those studies of WH biochar concerning its soil use were focused on some of the selected physicochemical properties of WH biochar. However, a more elaborated characterization of the biochar’s physicochemical properties induced by pyrolysis temperature needs to be investigated to have a broader view of WH biochar regarding its possible use as a soil amendment. Yet, studies on the production of biochar and its characteristics as a promising soil amendment from WH found in Lake Tana, Ethiopia, are barely available in the literature. Therefore, this work aimed to turn immensely available WH biomass into biochar and assess how the pyrolysis temperature alters the physicochemical characteristic of WH biochar as a soil amendment. The findings could provide insights into the management and utilization of WH biowaste for soil use by converting it into biochar through thermal treatment under various temperatures.

## 2 Materials and methods

### 2.1 Biomass collection and biochar production

The procedure of water hyacinth collection and preparation of biochar is presented in Fig. 1. WH biomass, used as a feedstock, was collected from Lake Tana, Ethiopia. Weed biomass was chopped into smaller pieces, washed with distilled water, and oven-dried at 105 °C to a uniform weight. After drying, the biomass was kept enclosed in an air-tight stainless-steel box with four small holes at the top of the cap to allow the

**Fig. 1** Steps of biochar production from water hyacinth. **a** Water hyacinth collected from Lake Tana. **b** Water hyacinth pyrolysis in different temperatures in an electric furnace. **c** Biochar produced from water hyacinth and crushing. **d** Biochar stored for analysis after sieving



produced gas to escape and positioned inside a muffle furnace (LT 40/12, Nabertherm GmbH, Germany). The biochar was prepared in three levels of pyrolysis temperatures (350 °C, 550 °C, and 750 °C) with a heating order of 5 °C/min and maintained at a specified temperature for 2 h. Following pyrolysis, the biochar was left inside the furnace to get cold. Then, finely ground biochar samples were sieved with a 2-mm sieve and collected in sealed bags, labeled WB350, WB550, and WB750, where WB stands for water hyacinth biochar and the numbers indicate the pyrolysis temperature.

## 2.2 Biochar characterization

### 2.2.1 Biochar yield and ash content

The yield of biochar was determined by the quotient of the weight of the produced biochar and the dried biomass used as a feedstock, and the result was expressed as a percentage (Eq. 1).

$$\text{Yield}(\%) = \frac{M_{\text{biochar}}}{M_{\text{biomass}}} \times 100 \quad (1)$$

where  $M_{\text{biochar}}$  is the weight of biochar (g), and  $M_{\text{biomass}}$  is the weight oven-dried biomass (g).

The amount of ash was measured following the American Society for Testing Materials (ASTM) method D1762-84. A 1 g of oven-dried biochar was ashed in a furnace at a heating rate of 5 °C/min and remained for 6 h at 750 °C, then a desiccator was used to cool the ash sample. The amount of ash was then calculated as described in Eq. 2:

$$\text{Ash}(\%) = \frac{M_{105} - M_{750}}{M_{105}} \times 100 \quad (2)$$

where  $M_{105}$  is the mass of oven-dried biochar at 105 °C and  $M_{750}$  is the residue that remained after ashing at 750 °C.

### 2.2.2 Elemental analysis

Biochar elemental compositions (C, H, N) were analyzed by applying the dry combustion method. The biochar sample ( $2 \pm 0.05$  mg) oven-dried at 105 °C overnight was encapsulated in an aluminum sample envelope. The sealed sample was subjected to dry combustion employing a CHN analyzer (2400 Series II, Perkin Elmer, USA). The oxygen (O) content was obtained by the calculation of  $100\% - (C + H + N + \text{Ash})\%$  [38]. The atomic mass ratios H/C and O/C were calculated from the elemental analysis result.

### 2.2.3 The pH, electrical conductivity, and cation exchange capacity

The pH and electrical conductivity (EC) of the biochar were determined at a biochar (g) to deionized water (mL) ratio of 1:10 [39]. The biochar and deionized water blend were placed in a horizontal shaker at a speed of 160 rpm for 1 h and the suspension was then left for half an hour. The pH and EC were determined from the suspension employing a calibrated pH meter (9625, JF25, Horiba Scientific, Japan) and an EC meter (Mettler-Toledo, USA). CEC was examined by adopting the standard described by Hien et al. [40]. In brief,  $1 \pm 0.05$  g biochar was combined in 40 mL of 1 M ammonium acetate (pH 7.0) and shaken for 15 h later on filtered through a 0.45- $\mu\text{m}$  filtrate membrane. Additionally, 50 mL of neutral pH 1 M ammonium acetate was used to wash the biochar. Then, 30 mL of ethanol was used to wash away the excess ammonium in the biochar. Then, 90 mL of 2 M KCl was applied to wash the biochar, and the filtrate was analyzed for  $\text{NH}_4^+$  to calculate biochar CEC using a flow injection autoanalyzer (FIALab 2500, USA).

### 2.2.4 Liming capacity

The liming potential of biochar samples was determined in line with Singh et al. [39], and the values were expressed as percent  $\text{CaCO}_3$  equivalence (CCE). Hence, 0.5 g of ground biochar blended with 10.0 mL of a standard 1 M HCl solution, shaken for 2 h, and then allowed to stand all night (16 h). Finally, using a standardized 0.5 M NaOH solution, the mixture was titrated under vigorous stirring until it reached a pH of 7. Then, the percent  $\text{CaCO}_3$  equivalence was determined using the calculation described in Singh et al. [39].

### 2.2.5 Available nutrients

A 2% formic acid extraction technique was used to determine the amount of available P present in the biochar [41]. A biochar sample weighing 0.35 g mixed with 35 mL of 2% formic acid was shaken at 160 rpm for half an hour. Then, after 10 min of centrifuging followed by filtration with Whatman No. 41 filter paper, the available P in the filtrate was measured with a flow injection autoanalyzer (FIALab 2500, USA). The 1 M HCl extraction procedure was used to determine the concentration of available Ca, Mg, and K [42]. A biochar sample (1 g) combined with 20 mL of 1 M HCl was shaken for 2 h and stood all night. Then, with Whatman No. 42 filter paper, the blend was filtered. The filtrate was later analyzed for K, Ca, and Mg using an atomic absorption spectrophotometer (PerkinElmer, USA).

### 2.2.6 Specific surface area and porosity

An analysis of biochar's specific surface area and porosity was done by applying the Brunauer–Emmett–Teller (BET) approach [43] through N adsorption–desorption isotherms (77 K) using an Accelerated Surface Area and Porosimetry (ASAP) (ASAP 2010, Micrometric, USA).

### 2.2.7 Surface functionality

To analyze biochar's surface functionality, a 1-mg sample of biochar was finely ground and well mixed with 100 mg KBr and pressed into a 13-mm pellet at a pressure of 7845 kPa. The spectra reading was undertaken with the help of IRAffinity-1S Fourier transform infrared spectroscopy (FTIR) (Shimadzu, Japan). Infrared absorbance data were attained for wavenumbers between 400 and 4000  $\text{cm}^{-1}$  at a spectral resolution of 2  $\text{cm}^{-1}$  with 64 scans [44].

### 2.2.8 Surface morphology and structure analysis

After drying a biochar sample for 24 h at 105 °C, surface morphology and structure imaging were examined using a

JEOL scanning electron microscope (SEM) (JSM-5600LV, USA). The dried biochar sample was coated on a carbon tap and fitted onto a sample holder for examination.

### 2.2.9 Water holding capacity

Biochar sample (1 g) previously oven-dried for a day at 105 °C was shaken for 2 h with distilled water to make sure all pores were filled with water. After shaking, the wet sample was left to drain on a funnel using Whatman No. 42 filter paper for 2 h. After draining, the drained biochar was weighed and spent 24 h in the oven at a temperature of 105 °C. Water-holding capacity (WHC) was then calculated by the weight of the water kept in the biochar sample per weight of the oven-dried biochar sample [38, 40].

## 2.3 Data analysis

Analysis of variance (ANOVA) was conducted to ascertain how the pyrolysis temperature influences WH biochar yield and physicochemical characteristics. Significant variations between means of various results were examined with the test of Tukey HSD at  $p < 0.05$  level of significance. The average of three replicates and the standard deviation were used to express the results. The homogeneity of variance was examined using Lavene's test. The whole statistical analysis was executed with SPSS version 26 software (SPSS Inc., Chicago). Graphs were plotted by employing Origin software (OriginLab, USA).

## 3 Results and discussion

### 3.1 Biochar yield, ash content, and elemental composition

Pyrolysis temperature impact on yield, ash content, and elemental compositions of WH biochar is presented in Table 1. The influence of pyrolysis temperature on the yield of biochar was significant ( $p < 0.05$ ). The rise of pyrolysis temperature from 350 to 750 °C resulted in a reduced yield of biochar from 51 to 33.3%, respectively. Previous studies also showed that the yield of biochar declined as pyrolysis temperature rose (Table 4). A larger reduction of the biochar yield (25.7%) was recorded between 350 and 550 °C, but the yield difference between 550 and 750 °C was lower (12.1%). The result aligned with 33 Zhang et al. [37] and Li et al. [45] who noted a declining yield of WH biochar during increasing pyrolysis temperature (Table 4). The reduction of biochar yield could be due to enhancing dehydration of biomass along with loss of volatile matter at higher pyrolytic temperatures [46]. Furthermore, an increase in temperature causes quick and thorough decomposition of lignocellulosic

**Table 1** Yield, ash content, elemental constituent, and atomic mass ratios of water hyacinth biochar produced at different pyrolysis temperatures

Biochar	Yield %	Ash	C	H	N	O	H/C	O/C	C/N
WB350	51.0±1.07 <sup>a</sup>	33.3±1.44 <sup>a</sup>	33.9±0.99 <sup>a</sup>	2.52±0.5 <sup>a</sup>	2.14±0.04 <sup>a</sup>	28.2±1.69 <sup>a</sup>	0.89±0.21 <sup>a</sup>	0.62±0.05 <sup>a</sup>	15.9±0.62 <sup>a</sup>
WB550	37.9±0.38 <sup>b</sup>	42.1±0.24 <sup>b</sup>	33.0±0.44 <sup>a</sup>	0.72±0.31 <sup>b</sup>	1.91±0.02 <sup>b</sup>	22.2±0.58 <sup>b</sup>	0.26±0.11 <sup>b</sup>	0.51±0.03 <sup>b</sup>	17.3±0.22 <sup>a</sup>
WB750	33.3±0.30 <sup>c</sup>	52.4±0.53 <sup>c</sup>	27.8±0.47 <sup>b</sup>	0.24±0.08 <sup>b</sup>	1.37±0.01 <sup>c</sup>	18.2±0.23 <sup>c</sup>	0.11±0.04 <sup>b</sup>	0.49±0.02 <sup>b</sup>	20.3±0.73 <sup>b</sup>

Results are presented with the mean±standard deviations ( $n=3$ ); numbers followed by the same letter in the same column are not significantly different ( $p<0.05$ )

constituents of the biomass that leads to a reduced char yield [47]. Reza et al. [48] also outlined a similar finding for an invasive grass *Pennisetum purpureum*.

The ash level of given biochar samples prepared under different temperatures of pyrolysis significantly ( $p<0.05$ ) varied among treatments. Raising the pyrolysis temperature increased the ash content significantly (Table 1). The ash levels found in this study were higher than in previous studies on WH biochar (Table 4). Bottezini et al. [32] reported a rise in the amount of ash (25.6–34.8%) for WH biochar during a temperature rise (400–600 °C). Similarly, in a pyrolysis temperature between 250 and 500 °C, the WH biochar ash concentration rose from 11.1 to 42.4% [49]. Likewise, in the research of Zhang et al. [37], the ash content in WH biochar increased from 34.8 to 43.0% as the temperature of pyrolysis rose between 350 and 550 °C. Dhar et al. [50] and Zhang et al. [51] also reported a rise in the ash content with pyrolysis temperature. The rise in ash content with temperature could be attributed to the volatilization of an organic matrix at higher pyrolysis temperatures [52]. Furthermore, the amount of ash present in a biochar depends on the feedstock's composition [53]. Compared to woody biomasses, biochar made from herbaceous biomasses had larger ash concentrations [54]. Additionally, a significant amount of ash from the current study biochar could be ascribed to the lower lignin content of WH biomass since WH is composed of 48% hemicellulose, 20% cellulose, and 3.5% lignin [34]. High lignin-containing biomass tends to yield high carbon biochar whereas low lignin-containing biomass results in high ash biochar [55]. Biochar with high ash amounts can be used as a fertilizer [56] and ameliorator of soil acidity [57]. Consequently, high levels of ash from WH biochar could serve as a source of minerals when added to the soil.

The current study's findings showed that the C, H, N, and ratios of H/C, O/C, and C/N were all significantly impacted ( $p<0.05$ ) by the pyrolysis temperature (Table 1). The C content significantly decreased as the pyrolysis temperature rose, which was opposite to the earlier reports on WH biochar (Table 4). The C proportion found in WB750 was significantly lower than WB350 and WB550. The diminishing C content of WH biochar with the rise in pyrolysis temperature could be ascribed to further decomposition and loss of

C due to high temperature. WB350 and WB550 may have a high percentage of aliphatic carbon and a low percentage of aromatic carbon [58]. Claoston et al. [59] claim that when the pyrolysis temperature rises, the level of carbonization diminishes and at high temperatures, C will be lost. When the pyrolysis temperature went up, H, N, and O contents showed a decreasing trend, which is consistent with Bottezini et al. [32] and Li et al. [45] who reported a depletion of biochar H, N, O, O/C, and H/C ratio for the WH biochar as the temperature of pyrolysis rose (Table 4). In the present study, the maximum reduction of H, N, and O was recorded with WB750. The existence of those elemental components in the form of CO, CO<sub>2</sub>, H<sub>2</sub>O, and hydrocarbons can be easily volatilized as pyrolysis temperature goes up [60]. Similarly, the ratio of H/C and O/C also declined with pyrolytic temperature. Temperature increase during pyrolysis induces H and O loss through rapid dehydration and decarboxylation reactions as it has developed condensed aromatic ring structures [61] and diminished functional groups containing the atoms O and H [55]. It has been demonstrated that the level of aromaticity rises as the charring temperature rises [62]. Accordingly, WB750 with a H/C ratio of 0.11 became highly carbonized forming higher aromaticity compared to WB350 and WB550. According to International Biochar Initiatives (IBI) guidelines [63], adding biochar to the soil that has a H/C ratio < 0.7 will effectively sequester carbon and persist for a longer time. Thus, WB550 and WB750 could be potential candidates for carbon sequestration.

The N content also significantly declined when the pyrolysis temperature rose. As there was a rise in temperature from 350 to 550 °C and 550 to 750 °C, the total N decreased by 12.0% and 39.4%, respectively. As Table 4 shows the N results were lower compared to N values reported by Bottezini et al. [32] and higher than values reported by Li et al. [45]. However, the C/N ratio escalates with the development of pyrolytic temperature. This result was supported by Bottezini et al. [32] who reported a comparable C/N value of WH biochar 16–23 for the 400–600 °C temperature range (Table 4). Narayanan et al. [49] also revealed a higher but decreasing C/N ratio (69.1–48.2) of WH biochar in a range of temperatures between 350 and 500 °C, owing to a high C level in their study (Table 4). Raising pyrolysis temperature

accelerates the disappearance of functional groups containing N [64]. Thus, the N depletion as the pyrolysis temperature rises increases the ratio of C to N [65]. The findings of the present investigation demonstrated the level of C decline was far lower than that of the decreasing rate of N, consequently leading to a greater C/N ratio for WH biochar at high temperatures. However, between WB350 and WB550, the C/N ratios were not significantly different. The ability of biochar to liberate inorganic N from organic matter once it enters the soil is frequently assessed using the C/N ratio [51]. Accordingly, WB350 and WB550 could release more inorganic N, when applied to the agricultural soil compared to WB550 and WB750.

### 3.2 Biochar pH, electrical conductivity, and cation exchange capacity

Water hyacinth biochar pH, EC, CEC, and liming potential results are provided in Table 2. The biochar pH changed substantially ( $p < 0.05$ ) among different temperatures with the highest pH (11.2) recorded for the WH biochar produced at 750 °C. The pH result indicated that all the samples were alkaline (9.24–11.2). High values of pH from WH biochar are parallel with the respective ash content of the biochar produced at a specified temperature (Table 1). The pH values reported in this study were higher than previous reports of biochar from WH (Table 4). The study's pH findings conform with the pH values (9.4–10.49) reported by Zhang et al. [37] for biochar derived from WH made between 250 and 550 °C. According to Liu et al. [66], the result of pH for WH biochar charred using temperatures in the range of 300–700 °C showed similar trends though the values were lower (7.3–7.6). Moreover, the results of pH results in this work agree with the pH values from the biochar produced from biomasses other than WH [67, 68]. The rise in pH of biochar along with temperature could be mainly caused by alkali salt buildup [69], an increase in the amount of ash [70], and with replacement of functional groups that are acidic by alkaline functional groups [71] during pyrolysis. Accordingly, biochar possessing a high pH can assist in soil acidity amelioration [55]. WH-derived biochar was reported to be a potential for soil acidity alleviation [36]. Hence, WH biochar could be used as a liming agent for low-pH tropical soils.

The mean values of EC in WH biochar developed at different temperatures were drastically ( $p < 0.05$ ) different, with the highest value of EC (44.7 mS cm<sup>-1</sup>) recorded for WB750. The EC values were consistent with the ash content of the given samples of WH biochar. Claoston et al. [59] reported that biochar's EC values grew as the pyrolysis temperature rose. Similarly, Zhang et al. [22] stated that EC values of biochar increased with pyrolysis temperature. Elevated temperature induces a higher loss of volatile matter that leads to a larger occurrence of minerals in the ash which consecutively raises the value of EC [72]. Given that K<sup>+</sup> ions are mobile, biochar with more mineral ash likely has a higher EC, particularly when compared to that with less mineral ash [73]. EC of biochar indicates the level of soluble salts present and is an essential factor manifesting the fertilizing effect of biochar [16]. Soil amendment with WH biochar should be taken into consideration owing to its higher mineral content that can improve soil fertility.

The CEC of WH biochar samples was found significantly ( $p < 0.05$ ) different owing to pyrolysis temperature. At 350 °C, the biochar CEC was highest, and at 750 °C, it was the lowest. When the pyrolysis temperature increased, the CEC value declined. This result was supported by the FTIR images where the functional groups substantially dropped as the temperature went up (Fig. 3). Zhang et al. [37] observed that the CEC for WH biochar produced at 450 °C and 550 °C, respectively, decreased from 21.95 to 14.23 cmol<sub>+</sub> kg<sup>-1</sup>. Likewise, Narayanan et al. [49] described a decreasing CEC value from 38.9 to 31.9 cmol<sub>+</sub> kg<sup>-1</sup> during an increase in pyrolysis temperature from 350 to 550 °C. The CEC result was found higher at lower temperatures compared to previous studies of WH biochar (Table 4). Correspondingly, Gaskin et al. [74] demonstrated a similar trend of decreasing CEC for 400 °C and 500 °C produced pine chip, peanut husk, and poultry litter biochars. At higher pyrolysis temperatures, the biochar tends to produce aromatic C and removes surface functional groups that lead to reduced CEC of biochar [75]. Raising the temperature of pyrolysis causes the disappearance of organic functional groups (-COO<sup>-</sup>, OH<sup>-</sup>) that primarily contribute to a particular biochar's CEC [65]. The CEC of a biochar strongly depends on the functional groups that contain oxygen on the biochar's surface [76]. Thus, the decrease in O levels in WH biochars as temperature increases (Table 1) might be

**Table 2** The pH, electrical conductivity, cation exchange capacity, and liming potential of water hyacinth biochar pyrolyzed at different temperatures

Biochar	pH	EC (mS cm <sup>-1</sup> )	CEC (cmol <sub>+</sub> kg <sup>-1</sup> )	Liming value (% CCE)
WB350	9.24 ± 0.007 <sup>a</sup>	28.0 ± 0.45 <sup>a</sup>	44.4 ± 0.65 <sup>a</sup>	17.7 ± 1.01 <sup>a</sup>
WB550	11.0 ± 0.005 <sup>b</sup>	32.9 ± 1.15 <sup>b</sup>	34.6 ± 1.67 <sup>b</sup>	24.8 ± 1.75 <sup>b</sup>
WB750	11.2 ± 0.003 <sup>c</sup>	44.7 ± 2.11 <sup>c</sup>	2.3 ± 0.14 <sup>c</sup>	33.0 ± 1.05 <sup>c</sup>

Means ± standard deviations (n=3) followed by similar letters across the column are not significantly different at  $p < 0.05$

a cause for a decrease in CEC values as temperature rises. Incorporation of biochar into the soil can enhance the fertility of the soil by improving the CEC and the soil's capacity to hold nutrients and minimizing soil acidity [4]. Based on the CEC results, WB350 and WB550 could be better used for the amendment of tropical soils having low CEC values.

### 3.3 Liming potential

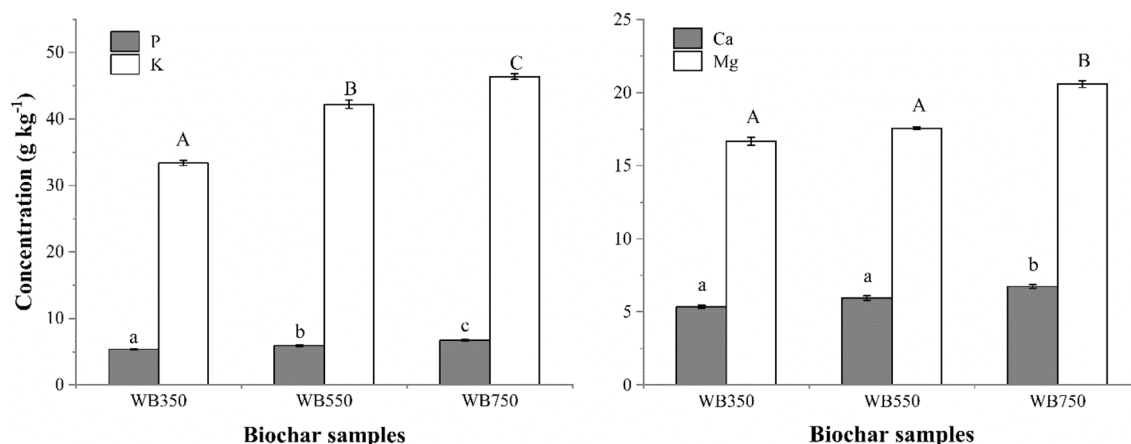
The liming potentials expressed as % CCE of WH biochar ranged from 17.7 to 33.0% (Table 2). The liming potentials of WH biochar produced at different temperatures significantly ( $p < 0.05$ ) varied. The findings revealed that WH biochar liming capacity increased as the pyrolysis temperature rose. Based on Camps-Arbestain et al. [42], the liming potential of WB350 was classified as class 2 (10–20% CCE), whereas WB550 and WB750 were classified as class 3 (> 20% CCE). The liming potential of WB350 and WB550 was lower compared to the green tomato waste biochar (33% CCE) [77] and paper mill waste biochar (29–33% CCE) [78] produced under a temperature of 550 °C through slow pyrolysis. High liming potentials of 72% and 86.3% CCE were reported for *E. Saligna* leaves and poultry litter biochars, respectively, produced in slow pyrolysis at 550 °C [79]. The ash content of a particular biochar plays a significant role in biochar's liming potential, but only to a considerably smaller extent by the pH [67]. In the current study, liming potential and ash content had a positive correlation (data not shown). Due to its alkalinity, ability to neutralize acidity, and high concentration of positive ions, biochar can be an ideal liming agent for soil acidity adjustment [80]. Accordingly, an acid soil amendment could be better developed from WH biochars especially generated at temperatures between 550 and 750 °C.

### 3.4 Available nutrients

Figure 2 shows a concentrated amount of available nutrients (P, K, Ca, and Mg) from WH biochar prepared under varying temperatures. The influence of pyrolysis temperature was ( $p < 0.05$ ) significant on the available P, Ca, Mg, and K contents of WH biochar. Increasing the pyrolysis temperature increased the concentration of nutrients. Maximum level of available P, Ca, Mg, and K was found in WB750. The findings of this study are in agreement with those of Gaskin et al. [74] and Wang et al. [81], who found that P, Ca, Mg, and K levels rose with rising temperature. Wang et al. [19] reported that the P and Ca concentrations in crop residue and wood biochar significantly increased as the temperature of pyrolysis rose from 500 to 700 °C. According to Bottezzini et al. [32], the total P content for WH biochar that was pyrolyzed at a temperature between 400 and 600 °C ranged from 7.23 to 7.56 g kg<sup>-1</sup> (Table 4). Phosphorous-rich biochar can be produced from WH since the ability of this aquatic weed plant to absorb large amounts of P is well documented [34]. Besides, pyrolysis temperature affects the volatilization properties and nutrient availability in biochar [82]. This study's findings also showed that WH biochar is rich in soil nutrients; hence, WH biochar can be a viable option for soil fertility amendment.

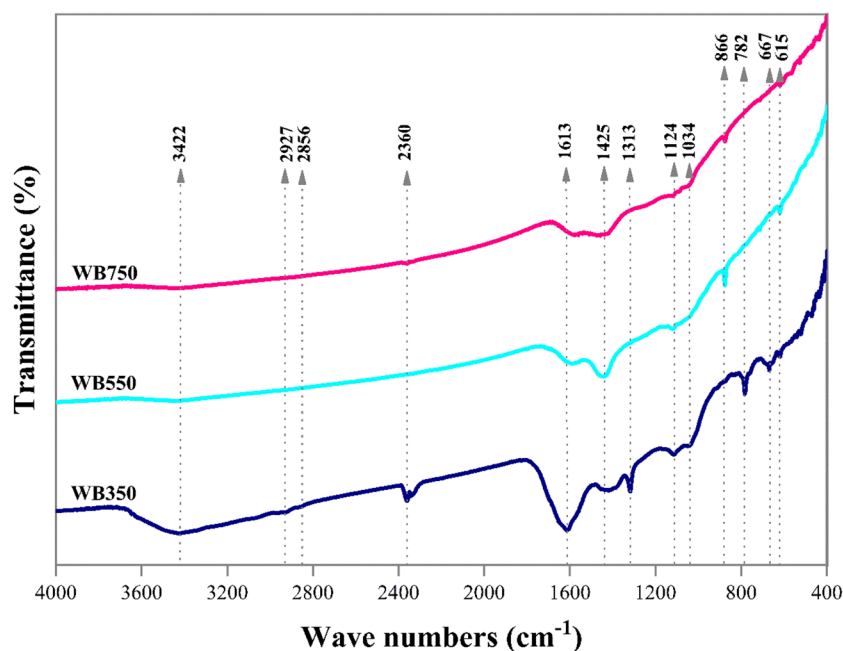
### 3.5 Surface functional groups

Figure 3 presents the FTIR spectra indicating the functional groups of WH biochar prepared under different temperatures. The broad band around 3422 cm<sup>-1</sup> could be due to the hydroxyl (O—H) group stretching, which became diminished as the temperature rose. The spectra around 2926–2864 cm<sup>-1</sup> on WB350 diminished as the temperature rose assigned to aliphatic CH stretching [83]. The



**Fig. 2** Concentration of available nutrients (P, K, Ca, Mg) in water hyacinth biochar produced at 350 °C (WB350), 550 °C (WB550), and 750 °C (WB750); vertical bars show standard error of means

**Fig. 3** Fourier transform infrared spectroscopy spectra of water hyacinth biochar produced at 350 °C (WB350), 550 °C (WB550), and 750 °C (WB750)



aliphatic CH groups break apart and reform into more aromatic thermostable forms of biochar as pyrolysis temperature increases [15]. The spectral band around 1613  $\text{cm}^{-1}$  assigned to the stretch of aromatic C=C and C=O of vinyl ethers [84, 85] was more visible on WB350 and WB550 but became lessened for WB750, which could be due to an increase in pyrolysis temperature that provided high energy to break double bonds [15]. A band around 1425  $\text{cm}^{-1}$  for WB350 and WB550, decreasing at WB750, could be associated with in-plane C—O—H bending [84]. The band around 1313  $\text{cm}^{-1}$  was observed only on the low-temperature biochar (WB350) and could be ascribed to the stretch of the C—O group [85]. The smaller band occurred around 1124  $\text{cm}^{-1}$  could be related to aliphatic ethers of C—O—C stretching and alcohol C—H bending [84]. For WB350, symmetric C—O stretching may be the cause of a band around 1034  $\text{cm}^{-1}$  [85, 86], and diminished as the temperature rose could be linked to the reduction of oxygen [86]. The spectral bands around 866 and 782  $\text{cm}^{-1}$  could be assigned to polynuclear aromatics from out-of-plane bending of C—H [85]. The bands below 665  $\text{cm}^{-1}$  could be assigned as aromatic rings [59]. As

illustrated in Fig. 3, a decrease in many FTIR peaks was observed when the pyrolysis temperature was increased from 350 to 750 °C. Overall, the decreasing values of O, H, and H/C and O/C ratios (Table 1) with increasing temperature hinted at a considerable removal of —OH and C—O containing polar functional groups [87]. The reduction of surface functional groups will have an impact on biochar's adsorption properties, where the CEC of biochar declines as temperature rises (Table 2). Regardless of the feedstock used, low-temperature biochar had more surface polar functional groups [15]. Thus, low-temperature biochars WB350 and WB550 could be applied to improve soil nutrient adsorption capability due to their relatively high surface functionality.

### 3.6 Surface area and pore characteristics

Table 3 displays the WH biochar's BET surface area, total pore volume, the volume of micropores, and the average width of pores. Figure 4 shows the nitrogen adsorption–desorption isotherms of the WH biochars obtained by different pyrolysis temperatures. With an increase in pyrolysis

**Table 3** Effect of varying pyrolysis temperatures on BET surface area, total pore volume, micropore volume, and average pore width of water hyacinth biochar

Biochar sample	BET surface area ( $\text{m}^2 \text{g}^{-1}$ )	Total pore volume ( $\text{cm}^3 \text{g}^{-1}$ )	Micropore volume ( $\text{cm}^3 \text{g}^{-1}$ )	Average pore width (nm)
WB350	1.1	0.00423	0.00158	15.4
WB550	14.6	0.01829	0.00349	5.01
WB750	29.8	0.03263	0.00601	4.37

WH biochar produced at different pyrolysis temperatures: WB350 (350 °C), WB550 (550 °C), and WB750 (750 °C)



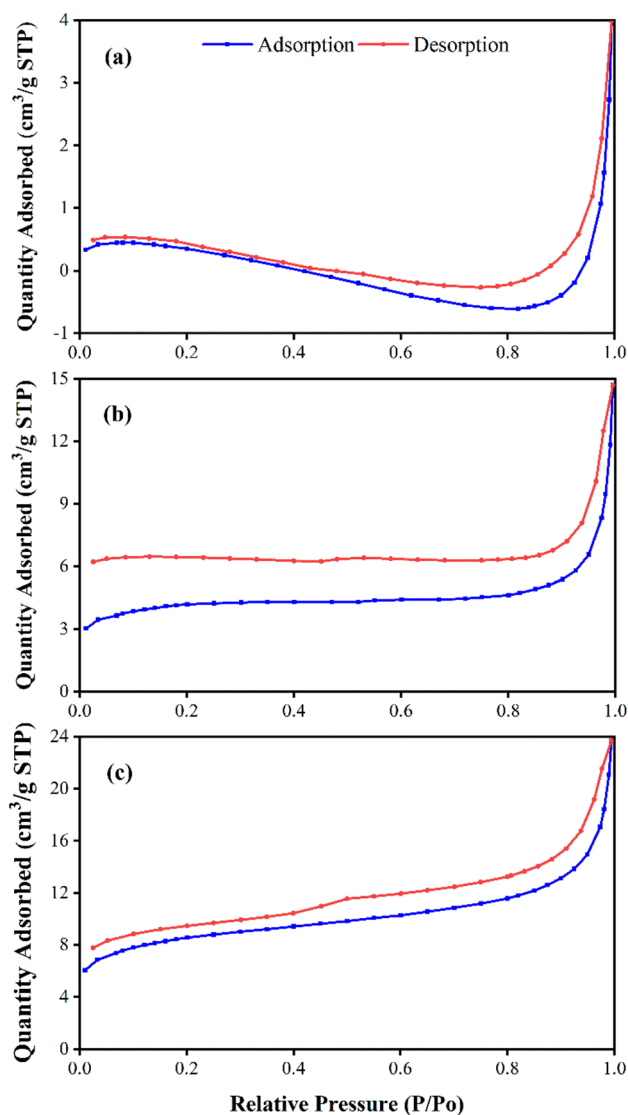


**Fig. 4** Nitrogen adsorption–desorption isotherms of WH biochars developed at (a) 350 °C, (b) 550 °C, and (c) 750 °C

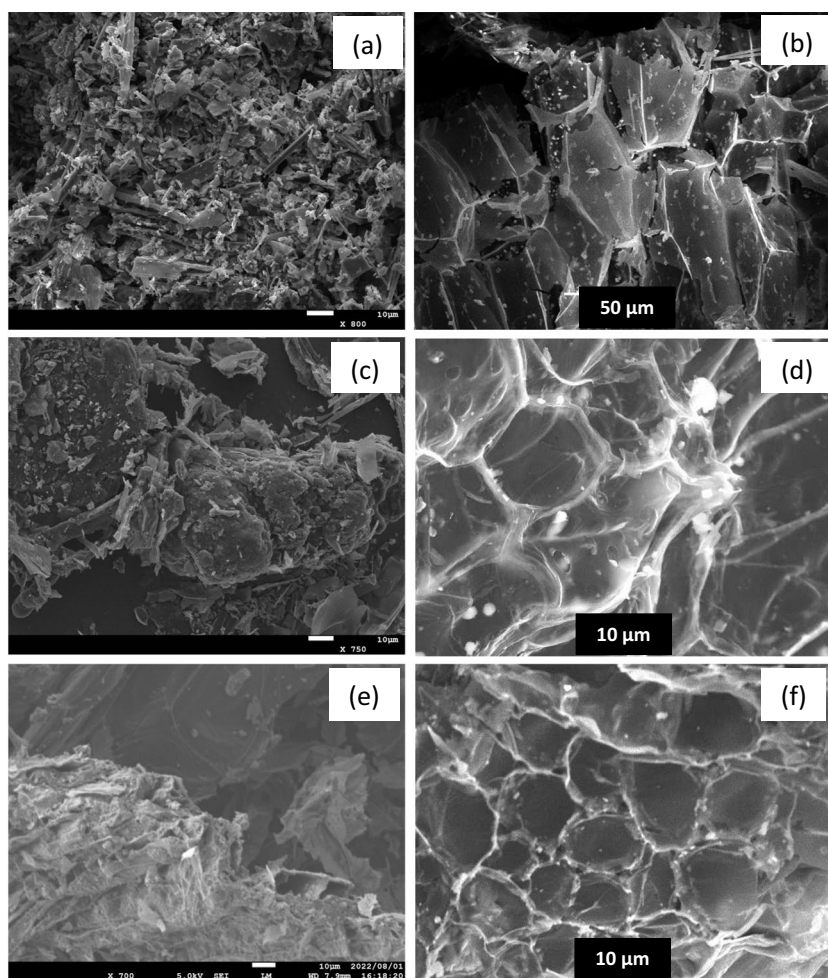
temperature BET surface area, total pore volume, and micropore volume increased, although the average width of pores decreased, which concurs with earlier research on WH biochar (Table 4). The size of pores and surface area results were supported with SEM images which showed that plenty of pores formed at higher temperatures (Fig. 5). Except for the lowest pyrolysis temperature (350 °C), the surface area results obtained from the current study appeared to be greater than those of WH biochar made at temperatures of 300 °C, 500 °C, and 700 °C with BET surface area of 2.5, 8.1, and 20.9 m<sup>2</sup> g<sup>-1</sup>, respectively [66]. However, higher values of BET surface area (175.5 m<sup>2</sup> g<sup>-1</sup>) and total pore volume (0.1183 cm<sup>3</sup> g<sup>-1</sup>) were reported by Li et al. [45] for WH biochar developed at a temperature of 700 °C (Table 4).

**Table 4** Comparison between values of the current and previous studies of WH biochar physicochemical properties derived under varying temperatures

Refer-ences	Pyrolysis tempera-ture (°C)	Yield (%)	Ash (%)	C (%)	H (%)	N (%)	O (%)	C/N	O/C	H/C	pH	P (g kg <sup>-1</sup> )	CEC (cmol <sub>c</sub> kg <sup>-1</sup> )	SSA (m <sup>2</sup> g <sup>-1</sup> )	TPV (cm <sup>3</sup> g <sup>-1</sup> )	Pore width (nm)
[32]	400–600	–	25.6–34.8	43.5–48.9	4.99–2.38	2.68–2.09	–	16–23	–	0.97–0.58	–	7.2–7.6	–	–	–	–
[35]	300~350	–	–	–	–	–	–	–	–	–	7.69	–	–	–	–	–
[36]	500	–	41.1*	–	–	–	–	–	–	–	7.62	18.09*	–	–	–	–
[37]	250–550	75.7–40.0	22.7–43.0	–	–	–	–	–	–	–	7.24–10.5	–	9.3–14.23	–	–	–
[45]	300–700	46.6–28.2	15.89–37.25	47.2–51.3	3.58–1.1	2.12–0.73	47.1–46.8	–	0.75–0.68	0.91–0.26	–	–	–	3.51–175.5	0.0005–0.071	7.7663–2.6971
[49]	350–500	33.6	11.1–42.4	39.2–72.5	–	–	–	69.1–48.2	–	–	–	0.16–0.29	38.9–31.9	–	–	–
[66]	300–700	–	–	–	–	–	–	–	–	–	7.3–7.6	–	–	2.5–20.9	–	56.6–39.3
[88]	900	–	–	–	–	–	–	–	–	–	–	–	–	25.9	0.0363	5.6014
This study	350–750	51.0–33.3	33.3–52.4	33.9–27.8	2.52–0.24	2.14–1.37	28.2–18.2	15.9–20.3	0.62–0.49	0.89–0.11	9.24–11.2	5.36–6.74	44.4–2.3	1.1–29.8	0.00423–0.03263	15.4–4.37

CEC, cation exchange capacity; SSA, specific surface area; TPV, total pore volume; \* average of the reported result

**Fig. 5** SEM-generated surface morphology images of water hyacinth biochar prepared at various pyrolysis temperatures. Biochar made at 350 °C (a) low magnification and (b) high magnification; biochar made at 550 °C (c) low magnification and (d) high magnification; biochar made at 750 °C (e) low magnification and (f) high magnification



In comparison to WB750, Allam et al. [88] reported a lower surface area ( $25.9 \text{ m}^2 \text{ g}^{-1}$ ) but a greater total pore volume ( $0.0363 \text{ cm}^3 \text{ g}^{-1}$ ) of WH biochar created at  $900 \text{ }^\circ\text{C}$  (Table 4). The surface area of the current study's biochar was found very low compared with wood biochar ( $347.8 \text{ m}^2 \text{ g}^{-1}$ ) and grass biochar ( $140.8 \text{ m}^2 \text{ g}^{-1}$ ) for the  $700 \text{ }^\circ\text{C}$  pyrolysis temperature [85], miscanthus ( $168\text{--}390 \text{ m}^2 \text{ g}^{-1}$ ), switchgrass ( $162\text{--}351 \text{ m}^2 \text{ g}^{-1}$ ), corn stover ( $149\text{--}357 \text{ m}^2 \text{ g}^{-1}$ ), and sugarcane bagasse ( $138\text{--}290 \text{ m}^2 \text{ g}^{-1}$ ) for pyrolysis temperature of  $500\text{--}800 \text{ }^\circ\text{C}$  [89]. Accordingly, improving the porosity and surface area of WH biochar as a soil amendment will be necessary. For instance, pyrolysis of WH with an activating agent,  $\text{ZnCl}_2$ , at  $600 \text{ }^\circ\text{C}$  produced a surface area of  $680.53\text{--}1199.3 \text{ m}^2 \text{ g}^{-1}$  and a total pore volume of  $0.33\text{--}1.88 \text{ cm}^3 \text{ g}^{-1}$  [90, 91]. This indicates that the addition of an activating agent during the pyrolysis of WH will enhance the surface area and porosity of biochar. The pore width of the present study biochar was higher than in earlier studies of WH biochar [45, 88]; however, the pore width reported by Liu et al. [66] was much larger than the present study results (Table 4).

During pyrolysis, the rate of cellulose and hemicellulose degradation increased as the temperature rose and this induced a higher biochar porosity and specific surface area [87]. Similarly, with increasing pyrolysis temperature, the loss of volatile matter will be higher resulting in the formation of a greater extent of micropores [92]. According to Kalderis et al. [93], biochar's surface area and porosity are among key properties for improving soil characteristics, such as its capacity to adsorb and retain water. Besides, the biochar's porous structures could function as a home ground for soil microbes [94] and as a site for soil nutrient adsorption [95]. Therefore, WH biochar could be an ideal material for improving the porosity of soil and increasing surface area for the adsorption of nutrients, water retention, soil aeration, and providing shelter for microbes.

### 3.7 Surface morphology and structure

Images of the surface morphology and structural details were taken employing SEM for WH biochar generated at

various temperatures. As illustrated in Fig. 5, the SEM images revealed that morphological changes were made at higher pyrolysis temperatures of 550 °C (Fig. 5c, d) and 750 °C (Fig. 5e, f). Well-arranged and porous structures were observed as the pyrolysis temperature rose, which may have been caused by the release of volatile matter that left more structured pores. In WB350, the SEM images (Fig. 5a, b) showed that the pores were not fully developed and filled up with volatile matter that remained inside cell structures. Results of WH biochar BET surface area and volume of the pore (Table 3) were consistent with the SEM images (Fig. 5).

Similar to this study's findings, Hu et al. [96] noted that increasing pyrolysis temperature caused WH biochar structural changes due to high temperature that resulted in increased porosity and surface area. As the pyrolysis temperature rose, the biochar's structure became more ordered and porous [59]. The macropores probably formed as a result of the raw biomass's vascular structures and the thermal decomposition process's loss of the cell wall's cellulose and hemicellulose [97]. Besides, multiple micropores developed due to the enhanced rate of devolatilization of volatile matter as temperature increased [92]. Considering the surface morphology and structure, biochar from WH could be a promising soil amendment to increase the soil's ability to store water and provide space for nutrient adsorption and soil microbes.

### 3.8 Water holding capacity

Pyrolysis temperature significantly ( $p < 0.05$ ) affected the WHC of the WH biochar samples (Fig. 6). The WHC of the sample biochars rose along with the pyrolysis temperature. The highest WHC recorded for WB750 was greater than WB350 and WB550 by 27.5% and 14.7%, respectively, whereas the WHC of WB550 was greater than WB350 by 11.2%. The increase in surface area and pore volume with temperature (Table 3) might be the reason for the elevated WHC of WH biochar, which is directly associated with the biochar's water retention property. Important factors that affect biochar's WHC include specific surface area and total volume of pores [98]. The results of the current study agreed with those of Hien et al. [40] who noted the WHC of bamboo biochar increased when the pyrolysis temperature rose from 400 to 800 °C. Moreover, it was claimed that using WH biochar on Brazil's sandy soils enhanced soil WHC [99]. According to Bordoloi et al. [35], adding WH biochar in a range from 0 to 15% by weight increased water retention by 29.5–48.5%, and available water content increased by 9.97 to 21.5% due to high porosity and hydrophilic property of biochar developed from WH. The present study result indicated that WH-derived biochar developed at 750 °C could be applied to reduce soil water stress of soils with low soil water holding capacity.

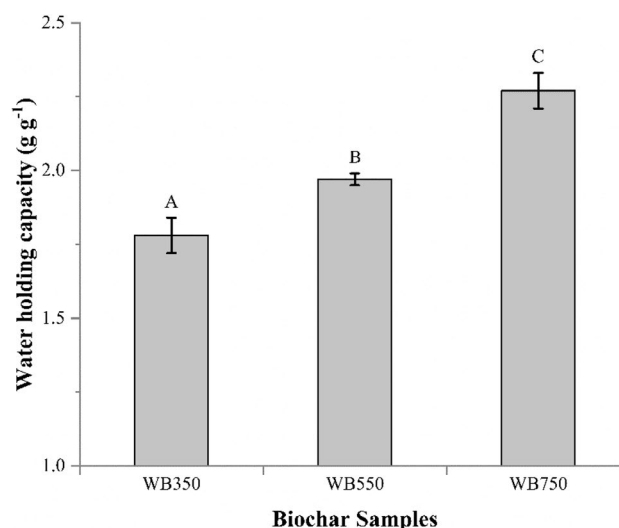


**Fig. 6** Pyrolysis temperature effect on water holding capacity of water hyacinth biochar derived at varying temperatures: WB350 (350 °C), WB550 (550 °C), WB750 (750 °C); error bars showed the standard error of the mean ( $n = 3$ )

### 3.9 Advantages of water hyacinth biochar for soil amendment

According to the findings, WH might be applied as an amendment to soil. The characteristics of each biochar, however, varied significantly and each demonstrated unique qualities for a particular role in soil amendment. Table 5 outlines the relative benefits of using WH biochars produced at varying temperatures, taking into account the yield and physicochemical properties of the resulting biochars.

## 4 Conclusion

The results revealed that pyrolysis temperature considerably influenced the physicochemical characteristics of water hyacinth biochar. Water hyacinth biochar developed at various pyrolysis temperatures exhibited distinct characteristics appropriate for specific functions in soil amendment. The alkaline nature of water hyacinth biochar samples could make use of soil acidity alleviation particularly developed at 550 °C and 750 °C. Water hyacinth biochar produced at 350 °C and 550 °C could be applied to improve low-pH agricultural soil's fertility and nutrient-holding capacity. Besides, biochar developed at 550 °C and 750 °C could be used for carbon sequestration. In addition, the biochar prepared at 750 °C could be used to improve soil water retention properties and porosity of soils. However, the surface area and porosity of WH biochar are very low. Adding activating agents during the pyrolysis of water hyacinth biowaste could

**Table 5** Relative advantages of water hyacinth biochar developed at various temperatures as a soil amendment

Advantages of WH biochar as a soil amendment	Relative order of advantages
i. Mass of production (yield)	WB350 > WB550 > WB750
ii. Soil acidity amendment	WB750 > WB550 > WB350
iii. Improvement of soil nutrient adsorption capacity	WB350 > WB550 > WB750
iv. Nitrogen supply (fertilizer effect)	WB350 > WB550 > WB750
v. Available nutrients (P and K) supply (fertilizer effect)	WB750 > WB550 > WB350
vii. Available nutrients (Ca and Mg) supply (fertilizer effect)	WB750 > WB550 ≈ WB350
viii. Ease of degradability by microbes (C/N ratio)	WB350 ≈ WB550 > WB750
ix. Aromaticity (H/C and O/C ratio)	WB750 ≈ WB550 > WB350
x. Long-term persistence in the soil (carbon sequestration)	WB750 ≈ WB550 > WB350
xi. Improvement of soil physical properties (water holding capacity, aeration, porosity)	WB750 > WB550 > WB350
xii. Providing space for microbes	WB750 > WB550 > WB350

Water hyacinth biochar developed at 350 °C (WB350), 550 °C (WB550), and 750 °C (WB750)

be an option to improve the surface area and porosity of water hyacinth biochar. By employing different pyrolysis temperatures, suitable biochar properties for soil use can be obtained from water hyacinth biowaste. Moreover, the conversion of water hyacinth biowaste into biochar can be an alternative mechanism for controlling weed infestation and waste utilization. Biochar characteristics indicate a biochar's capability to amend soil; however, the characteristics alone cannot assure soil quality amendment using biochar. Therefore, future studies should focus on verifying soil amelioration and agronomic effectiveness of biochar developed from water hyacinth at different pyrolysis temperatures in a field setting.

**Acknowledgements** Professor Shinjiro Sato's lab members from the Faculty of Science and Engineering at Soka University, Japan, who helped with the biochar analysis, are highly acknowledged by the authors. The Ethiopian Lake Tana and Other Water Bodies Authority is dully acknowledged for granting access to the water hyacinth at Lake Tana.

**Author contribution** Ashenafei Gezahegn: conceptualization; methodology; formal analysis and investigation; writing—original draft preparation. Yihenew G. Selassie: conceptualization; methodology; supervision; writing—review and editing. Getachew Agegnehu: conceptualization; methodology; supervision; writing—review and editing. Solomon Addisu: conceptualization; methodology; supervision; funding acquisition; resources; writing—review and editing. Fekremariam Asargew Mihretie: conceptualization; methodology; writing—review and editing. Yudai Kohira: methodology; formal analysis and investigation; writing—review and editing. Shinjiro Sato: conceptualization; methodology; funding acquisition; formal analysis and investigation; resources; supervision; writing—review and editing.

**Funding** This research was supported by Plankton Ecoengineering for Environment and Economic Transformations project, which was funded by MEXT/Japan, and the Project for Eco-Engineering for Agricultural Revitalization toward Improvement of Human Nutrition/EARTH: Water Hyacinth to Energy and Agricultural Crops funded by the Japan Science and Technology Agency/JST and Japan International

Cooperation Agency/JICA under Japan Science and Technology Research Partnership for Sustainable Development/SATREPS (grant number—JPMJSA2005).

**Data availability** The data used in this study are available within the article.

## Declarations

**Ethical** This declaration is not applicable.

**Competing interests** The authors declare no competing interests.

## References

- Lehmann J, Joseph S (2015) Biochar for environmental management: science, technology and implementation. Routledge. <https://doi.org/10.4324/9780203762264>
- Paz-Ferreiro J, Gascó G, Gutiérrez B, Méndez A (2011) Soil biochemical activities and the geometric mean of enzyme activities after application of sewage sludge and sewage sludge biochar to soil. *Biol Fertil Soils* 48:511–517. <https://doi.org/10.1007/s00374-011-0644-3>
- Ding Y, Liu Y, Liu S, Li Z, Tan X, Huang X, Zeng G, Zhou L, Zheng B (2016) Biochar to improve soil fertility. *Agron Sustain Dev* 36:1–18. <https://doi.org/10.1007/s13593-016-0372-z>
- Agegnehu G, Nelson PN, Bird MI (2016) Crop yield, plant nutrient uptake and soil physicochemical properties under organic soil amendments and nitrogen fertilization on Nitisols. *Soil Tillage Res* 160:1–13. <https://doi.org/10.1016/j.still.2016.02.003>
- Yf Y, He Xh, Gao R, Hl Ma, Ys Y (2014) Effects of rice straw and its biochar addition on soil labile carbon and soil organic carbon. *J Integr Agric* 13:491–498. [https://doi.org/10.1016/s2095-3119\(13\)60704-2](https://doi.org/10.1016/s2095-3119(13)60704-2)
- Pandit NR, Mulder J, Hale SE, Zimmerman AR, Pandit BH, Cornelissen G (2018) Multi-year double cropping biochar field trials in Nepal: finding the optimal biochar dose through agronomic trials and cost-benefit analysis. *Sci Total Environ* 637–638:1333–1341. <https://doi.org/10.1016/j.scitotenv.2018.05.107>

7. Pokharel P, Ma Z, Chang SX (2020) Biochar increases soil microbial biomass with changes in extra- and intracellular enzyme activities: a global meta-analysis. *Biochar* 2:65–79. <https://doi.org/10.1007/s42773-020-00039-1>
8. Karimi A, Moezzi A, Chorom M, Enayatizamir N (2020) Application of biochar changed the status of nutrients and biological activity in a calcareous soil. *J Soil Sci Plant Nutr* 20:450–459. <https://doi.org/10.1007/s42729-019-00129-5>
9. Verheijen FGA, Zhuravel A, Silva FC, Amaro A, Ben-Hur M, Keizer JJ (2019) The influence of biochar particle size and concentration on bulk density and maximum water holding capacity of sandy vs sandy loam soil in a column experiment. *Geoderma* 347:194–202. <https://doi.org/10.1016/j.geoderma.2019.03.044>
10. Baiamonte G, Crescimanno G, Parrino F, De Pasquale C (2019) Effect of biochar on the physical and structural properties of a sandy soil. *CATENA* 175:294–303. <https://doi.org/10.1016/j.catena.2018.12.019>
11. Atkinson CJ, Aitkenhead M (2018) How good is the evidence that soil-applied biochar improves water-holding capacity? *Soil Use Manag* 34:177–186. <https://doi.org/10.1111/sum.12413>
12. Hale SE, Alling V, Martinsen V, Mulder J, Breedveld GD, Cornelissen G (2013) The sorption and desorption of phosphate-P, ammonium-N and nitrate-N in cacao shell and corn cob biochars. *Chemosphere* 91:1612–1619. <https://doi.org/10.1016/j.chemosphere.2012.12.057>
13. Ye L, Camps-Arbestain M, Shen Q, Lehmann J, Singh B, Sabir M, Condron LM (2020) Biochar effects on crop yields with and without fertilizer: a meta-analysis of field studies using separate controls. *Soil Use Manag* 36:2–18. <https://doi.org/10.1111/sum.12546>
14. Uras Ü, Carrier M, Hardie AG, Knoetze JH (2012) Physico-chemical characterization of biochars from vacuum pyrolysis of South African agricultural wastes for application as soil amendments. *J Anal Appl Pyrol* 98:207–213. <https://doi.org/10.1016/j.jaap.2012.08.007>
15. Li S, Chen G (2018) Thermogravimetric, thermochemical, and infrared spectral characterization of feedstocks and biochar derived at different pyrolysis temperatures. *Waste Manag* 78:198–207. <https://doi.org/10.1016/j.wasman.2018.05.048>
16. Balmuk G, Videgain M, Manyà JJ, Duman G, Yanik J (2023) Effects of pyrolysis temperature and pressure on agronomic properties of biochar. *J Anal Appl Pyrol* 169. <https://doi.org/10.1016/j.jaap.2023.105858>
17. Tomczyk A, Sokołowska Z, Boguta P (2020) Biochar physico-chemical properties: pyrolysis temperature and feedstock kind effects. *Rev Environ Sci Biotechnol* 19:191–215. <https://doi.org/10.1007/s11157-020-09523-3>
18. Guo J, Zheng L, Li Z, Zhou X, Cheng S, Zhang L, Zhang Q (2021) Effects of various pyrolysis conditions and feedstock compositions on the physicochemical characteristics of cow manure-derived biochar. *J Clean Prod* 311:127458. <https://doi.org/10.1016/j.jclepro.2021.127458>
19. Wang Y, Hu Y, Zhao X, Wang S, Xing G (2013) Comparisons of biochar properties from wood material and crop residues at different temperatures and residence times. *Energy Fuels* 27:5890–5899. <https://doi.org/10.1021/ef400972z>
20. Sun Y, Gao B, Yao Y, Fang J, Zhang M, Zhou Y, Chen H, Yang L (2014) Effects of feedstock type, production method, and pyrolysis temperature on biochar and hydrochar properties. *Chem Eng J* 240:574–578. <https://doi.org/10.1016/j.cej.2013.10.081>
21. Sohi S, Lopez-Capel E, Krull E, Bol R (2009) Biochar, climate change and soil: a review to guide future research. *CSIRO Land and Water Sci. Rep* 5:17–31
22. Zhang Z, Zhu Z, Shen B, Liu L (2019) Insights into biochar and hydrochar production and applications: a review. *Energy* 171:581–598. <https://doi.org/10.1016/j.energy.2019.01.035>
23. Ahmed A, Abu Bakar MS, Hamdani R, Park YK, Lam SS, Sukri RS, Hussain M, Majeed K, Phusunti N, Jamil F, Aslam M (2020) Valorization of underutilized waste biomass from invasive species to produce biochar for energy and other value-added applications. *Environ Res* 186:109596. <https://doi.org/10.1016/j.envres.2020.109596>
24. Villamagna AM, Murphy BR (2010) Ecological and socio-economic impacts of invasive water hyacinth (*Eichhornia crassipes*): a review. *Freshw Biol* 55:282–298. <https://doi.org/10.1111/j.1365-2427.2009.02294.x>
25. Firehun Y, Struik P, Lantinga E, Taye T (2013) Joint use of insects and fungal pathogens in the management of water hyacinth (*Eichhornia crassipes*): perspectives for Ethiopia. *J Aquat Plant Manage* 51:109–121
26. Wassie A, Minwuyelet M, Ayalew W, Dereje T, Woldegebrael WK, Addisalem A, Wondie E (2014) Water hyacinth coverage survey report on Lake Tana. Tech Rep Ser I. [https://www.bdu.edu.et/sites/default/files/publication/Water\\_Hyacinth\\_Lake%20Tana\\_Report%20Series%201.pdf](https://www.bdu.edu.et/sites/default/files/publication/Water_Hyacinth_Lake%20Tana_Report%20Series%201.pdf)
27. Dersseh MG, Melesse AM, Tilahun SA, Abate M, Dagnaw DC (2019) Water hyacinth: review of its impacts on hydrology and ecosystem services—lessons for management of Lake Tana. *Extreme hydrology and climate variability*, pp 237–251. <https://doi.org/10.1016/B978-0-12-815998-9.00019-1>
28. Tewabe D, Asmare E, Zelalem W, Mohamed B (2017) Identification of impacts, some biology of water hyacinth (*Eichhornia crassipes*) and its management options in Lake Tana, Ethiopia. *Net J Agric Sci* 5:8–15
29. Enyew BG, Assefa WW, Gezie A (2020) Socioeconomic effects of water hyacinth (*Eichhornia crassipes*) in Lake Tana. *PLoS One* 15:e0237668. <https://doi.org/10.1371/journal.pone.0237668>
30. Gezie A, Assefa WW, Getnet B, Anteneh W, Dejen E, Mereta ST (2018) Potential impacts of water hyacinth invasion and management on water quality and human health in Lake Tana watershed, Northwest Ethiopia. *Biol Invasions* 20:2517–2534. <https://doi.org/10.1007/s10530-018-1717-0>
31. Maruyama DO, Si A, Sekine M, Fujita A, Habtu NG, Sato S, Toda T (2023) Enhancement of water hyacinth juice treatment in an anaerobic sequential batch reactor with coffee husk-derived biochar. *Bioenergy Res*. <https://doi.org/10.1007/s12155-023-10593-8>
32. Bottezini L, Dick DP, Wisniewski A, Knicker H, Carregosa ISC (2021) Phosphorus species and chemical composition of water hyacinth biochars produced at different pyrolysis temperature. *Bioresour Technol Rep* 14:1–8. <https://doi.org/10.1016/j.biteb.2021.100684>
33. Mastro RE, Kumar S, Rout TK, Sarkar P, George J, Ram LC (2013) Biochar from water hyacinth (*Eichhornia crassipes*) and its impact on soil biological activity. *CATENA* 111:64–71. <https://doi.org/10.1016/j.catena.2013.06.025>
34. Sindhu R, Binod P, Pandey A, Madhavan A, Alphonsa JA, Vivek N, Gnansounou E, Castro E, Faraco V (2017) Water hyacinth a potential source for value addition: an overview. *Bioresour Technol* 230:152–162. <https://doi.org/10.1016/j.biortech.2017.01.035>
35. Bordoloi S, Garg A, Sreedeeep S, Lin P, Mei G (2018) Investigation of cracking and water availability of soil-biochar composite synthesized from invasive weed water hyacinth. *Bioresour Technol* 263:665–677. <https://doi.org/10.1016/j.biortech.2018.05.011>
36. Jutakanoke R, Intaravicha N, Charoensuksai P, Mhuantong W, Boonnorat J, Sichaem J, Phongsopitanun W, Chakritbudsabong W, Rungarunlert S (2023) Alleviation of soil acidification and modification of soil bacterial community by biochar derived from water hyacinth *Eichhornia crassipes*. *Sci Rep* 13:397. <https://doi.org/10.1038/s41598-023-27557-9>
37. Zhang F, Wang X, Yin D, Peng B, Tan C, Liu Y, Tan X, Wu S (2015) Efficiency and mechanisms of Cd removal from aqueous solution by biochar derived from water hyacinth (*Eichhornia*

- crassipes). *J Environ Manage* 153:68–73. <https://doi.org/10.1016/j.jenvman.2015.01.043>
38. Mimmo T, Panzacchi P, Baratieri M, Davies CA, Tonon G (2014) Effect of pyrolysis temperature on miscanthus (*Miscanthus × giganteus*) biochar physical, chemical and functional properties. *Biomass Bioenerg* 62:149–157. <https://doi.org/10.1016/j.biombioe.2014.01.004>
  39. Singh B, Dolk MM, Shen Q, Camps-Arbestain M (2017) Biochar pH, electrical conductivity and liming potential. In: Singh B, Camps-Arbestain M, Lehmann J (eds) *Biochar: a guide to analytical methods*. CRC Press/Taylor and Francis Group LLC, pp 23–38
  40. Hien TTT, Tsubota T, Taniguchi T, Shinogi Y (2020) Enhancing soil water holding capacity and provision of a potassium source via optimization of the pyrolysis of bamboo biochar. *Biochar* 3:51–61. <https://doi.org/10.1007/s42773-020-00071-1>
  41. Wang T, Camps-Arbestain M, Hedley M, Bishop P (2012) Predicting phosphorus bioavailability from high-ash biochars. *Plant Soil* 357:173–187. <https://doi.org/10.1007/s11104-012-1131-9>
  42. Camps-Arbestain M, Amonette JE, Singh B, Wang T, Schmidt HP (2015) A biochar classification system and associated test methods. In: Lehmann J, Joseph S (eds) *Biochar for environmental management: science, technology and implementation*. Routledge, pp 165–193
  43. Brunauer S, Emmett PH, Teller E (1938) Adsorption of gases in multimolecular layers. *J Am Chem Soc* 60:309–319
  44. Ahmed M, Nigussie A, Addisu S, Belay B, Sato S (2021) Valorization of animal bone into phosphorus biofertilizer: effects of animal species, thermal processing method, and production temperature on phosphorus availability. *Soil Sci. Plant Nutr* 67:471–481. <https://doi.org/10.1080/00380768.2021.1945403>
  45. Li F, Shen K, Long X, Wen J, Xie X, Zeng X, Liang Y, Wei Y, Lin Z, Huang W, Zhong R (2016) Preparation and characterization of biochars from *Eichhornia crassipes* for cadmium removal in aqueous solutions. *PLoS ONE* 11:e0148132. <https://doi.org/10.1371/journal.pone.0148132>
  46. Mašek O, Brownsort P, Cross A, Sohi S (2013) Influence of production conditions on the yield and environmental stability of biochar. *Fuel* 103:151–155. <https://doi.org/10.1016/j.fuel.2011.08.044>
  47. Novak JM, Lima I, Xing B, Gaskin JW, Steiner C, Das K, Ahmedna M, Rehrh D, Watts DW, Busscher WJ (2009) Characterization of designer biochar produced at different temperatures and their effects on a loamy sand. *Ann Reg Sci* 3:195–206
  48. Reza MS, Afroze S, Bakar MSA, Saidur R, Asliffattahi N, Taweekun J, Azad AK (2020) Biochar characterization of invasive *Pennisetum purpureum* grass: effect of pyrolysis temperature. *Biochar* 2:239–251. <https://doi.org/10.1007/s42773-020-00048-0>
  49. Narayanan M, Kandasamy G, Kandasamy S, Natarajan D, Devarayan K, Alsehli M, Elfaskhany A, Pugazhendhi A (2021) Water hyacinth biochar and *Aspergillus niger* biomass amalgamation potential in removal of pollutants from polluted lake water. *J Environ Chem Eng* 9:105574. <https://doi.org/10.1016/j.jece.2021.105574>
  50. Dhar SA, Sakib TU, Hilary LN (2022) Effects of pyrolysis temperature on production and physicochemical characterization of biochar derived from coconut fiber biomass through slow pyrolysis process. *Biomass Convers Biorefin* 12:2631–2647. <https://doi.org/10.1007/s13399-020-01116-y>
  51. Zhang X, Zhao B, Liu H, Zhao Y, Li L (2022) Effects of pyrolysis temperature on biochar's characteristics and speciation and environmental risks of heavy metals in sewage sludge biochars. *Environ Technol Innov* 26. <https://doi.org/10.1016/j.eti.2022.102288>
  52. Lataf A, Jozefczak M, Vandecasteele B, Viaene J, Schreurs S, Carleer R, Yperman J, Marchal W, Cuypers A, Vandamme D (2022) The effect of pyrolysis temperature and feedstock on biochar agronomic properties. *J Anal Appl Pyrol* 168:105728. <https://doi.org/10.1016/j.jaap.2022.105728>
  53. Zhang X, Zhang P, Yuan X, Li Y, Han L (2020) Effect of pyrolysis temperature and correlation analysis on the yield and physicochemical properties of crop residue biochar. *Bioresour Technol* 296:122318. <https://doi.org/10.1016/j.biortech.2019.122318>
  54. Tu P, Zhang G, Wei G, Li J, Li Y, Deng L, Yuan H (2022) Influence of pyrolysis temperature on the physicochemical properties of biochars obtained from herbaceous and woody plants. *Bioresour Bioprocess* 9:131. <https://doi.org/10.1186/s40643-022-00618-z>
  55. Windeatt JH, Ross AB, Williams PT, Forster PM, Nahil MA, Singh S (2014) Characteristics of biochars from crop residues: potential for carbon sequestration and soil amendment. *J Environ Manage* 146:189–197. <https://doi.org/10.1016/j.jenvman.2014.08.003>
  56. He X, Liu Z, Niu W, Yang L, Zhou T, Qin D, Niu Z, Yuan Q (2018) Effects of pyrolysis temperature on the physicochemical properties of gas and biochar obtained from pyrolysis of crop residues. *Energy* 143:746–756. <https://doi.org/10.1016/j.energy.2017.11.062>
  57. Rodriguez JA, Filho JFL, Melo LCA, de Assis IR, de Oliveira TS (2020) Influence of pyrolysis temperature and feedstock on the properties of biochars produced from agricultural and industrial wastes. *J Anal Appl Pyrol* 149:104839. <https://doi.org/10.1016/j.jaap.2020.104839>
  58. McBeath AV, Smernik RJ (2009) Variation in the degree of aromatic condensation of chars. *Org Geochem* 40:1161–1168. <https://doi.org/10.1016/j.orggeochem.2009.09.006>
  59. Claoston N, Samsuri AW, Husni MHA, Amran MSM (2014) Effects of pyrolysis temperature on the physicochemical properties of empty fruit bunch and rice husk biochars. *Waste Manag Res* 32:331–339. <https://doi.org/10.1177/0734242X14525822>
  60. Jin J, Li Y, Zhang J, Wu S, Cao Y, Liang P, Zhang J, Wong MH, Wang M, Shan S, Christie P (2016) Influence of pyrolysis temperature on properties and environmental safety of heavy metals in biochars derived from municipal sewage sludge. *J Hazard Mater* 320:417–426. <https://doi.org/10.1016/j.jhazmat.2016.08.050>
  61. Wu W, Yang M, Feng Q, McGrouther K, Wang H, Lu H, Chen Y (2012) Chemical characterization of rice straw-derived biochar for soil amendment. *Biomass Bioenerg* 47:268–276. <https://doi.org/10.1016/j.biombioe.2012.09.034>
  62. Nguyen BT, Lehmann J, Hockaday WC, Joseph S, Masiello CA (2010) Temperature sensitivity of black carbon decomposition and oxidation. *Environ Sci Technol* 44:3324–3331. <https://doi.org/10.1021/es903016y>
  63. International Biochar Initiatives (IBI) (2015) Standardized product definition and product testing guidelines for biochar that is used in soil version 2.1. [https://biochar-international.org/wp-content/uploads/2023/01/IBI\\_Biochar\\_Standards\\_V2.1\\_Final2.pdf](https://biochar-international.org/wp-content/uploads/2023/01/IBI_Biochar_Standards_V2.1_Final2.pdf)
  64. Chen D, Yin L, Wang H, He P (2014) Pyrolysis technologies for municipal solid waste: a review. *Waste Manag* 34:2466–2486. <https://doi.org/10.1016/j.wasman.2014.08.004>
  65. Yuan JH, Xu RK, Zhang H (2011) The forms of alkalis in the biochar produced from crop residues at different temperatures. *Bioresour Technol* 102:3488–3497. <https://doi.org/10.1016/j.biortech.2010.11.018>
  66. Liu C, Ye J, Lin Y, Wu J, Price GW, Burton D, Wang Y (2020) Removal of cadmium (II) using water hyacinth (*Eichhornia crassipes*) biochar alginate beads in aqueous solutions. *Environ Pollut* 264:114785. <https://doi.org/10.1016/j.envpol.2020.114785>
  67. Domingues RR, Trugilho PF, Silva CA, Melo I, Melo LCA, Magriotis ZM, Sanchez-Monedero MA (2017) Properties of biochar derived from wood and high-nutrient biomasses with the aim of agronomic and environmental benefits. *PLoS ONE* 12:e0176884. <https://doi.org/10.1371/journal.pone.0176884>

68. Chin-Pampillo JS, Alfaro-Vargas A, Rojas R, Giacomelli CE, Perez-Villanueva M, Chinchilla-Soto C, Alcañiz JM, Domene X (2020) Widespread tropical agrowastes as novel feedstocks for biochar production: characterization and priority environmental uses. *Biomass Convers Biorefin* 11:1775–1785. <https://doi.org/10.1007/s13399-020-00714-0>
69. Ding W, Dong X, Ime IM, Gao B, Ma LQ (2014) Pyrolytic temperatures impact lead sorption mechanisms by bagasse biochars. *Chemosphere* 105:68–74. <https://doi.org/10.1016/j.chemosphere.2013.12.042>
70. Zhao L, Cao X, Masek O, Zimmerman A (2013) Heterogeneity of biochar properties as a function of feedstock sources and production temperatures. *J Hazard Mater* 256–257:1–9. <https://doi.org/10.1016/j.jhazmat.2013.04.015>
71. Al-Wabel MI, Al-Omran A, El-Naggar AH, Nadeem M, Usman AR (2013) Pyrolysis temperature induced changes in characteristics and chemical composition of biochar produced from cono-carpus wastes. *Bioresour Technol* 131:374–379. <https://doi.org/10.1016/j.biortech.2012.12.165>
72. Cantrell KB, Hunt PG, Uchimiya M, Novak JM, Ro KS (2012) Impact of pyrolysis temperature and manure source on physico-chemical characteristics of biochar. *Bioresour Technol* 107:419–428. <https://doi.org/10.1016/j.biortech.2011.11.084>
73. Joseph S, Downie A, Munroe P, Crosky A, Lehmann J (2007) Biochar for carbon sequestration, reduction of greenhouse gas emissions and enhancement of soil fertility; a review of the materials science. [https://www.researchgate.net/profile/Johannes-Lehmann-5/publication/228483265\\_Biochar\\_for\\_Carbon\\_Sequestration\\_Reduction\\_of\\_Greenhouse\\_Gas\\_Emissions\\_and\\_Enhancement\\_of\\_Soil\\_Fertility\\_A\\_Review\\_of\\_the\\_Materials\\_Science/links/53f501d20cf288a74913ba8/Biochar-for-Carbon-Sequestration-Reduction-of-Greenhouse-Gas-Emissions-and-Enhancement-of-Soil-Fertility-A-Review-of-the-Materials-Science.pdf](https://www.researchgate.net/profile/Johannes-Lehmann-5/publication/228483265_Biochar_for_Carbon_Sequestration_Reduction_of_Greenhouse_Gas_Emissions_and_Enhancement_of_Soil_Fertility_A_Review_of_the_Materials_Science/links/53f501d20cf288a74913ba8/Biochar-for-Carbon-Sequestration-Reduction-of-Greenhouse-Gas-Emissions-and-Enhancement-of-Soil-Fertility-A-Review-of-the-Materials-Science.pdf)
74. Gaskin JW, Steiner C, Harris K, Das KC, Bibens B (2008) Effect of low-temperature pyrolysis conditions on biochar for agricultural use. *Transactions of the ASABE* 51:2061–2069. <https://doi.org/10.13031/2013.25409>
75. Zornoza R, Moreno-Barriga F, Acosta JA, Munoz MA, Faz A (2016) Stability, nutrient availability and hydrophobicity of biochars derived from manure, crop residues, and municipal solid waste for their use as soil amendments. *Chemosphere* 144:122–130. <https://doi.org/10.1016/j.chemosphere.2015.08.046>
76. Banik C, Lawrinenko M, Bakshi S, Laird DA (2018) Impact of pyrolysis temperature and feedstock on surface charge and functional group chemistry of biochars. *J Environ Qual* 47:452–461. <https://doi.org/10.2134/jeq2017.11.0432>
77. Smider B, Singh B (2014) Agronomic performance of a high ash biochar in two contrasting soils. *Agr Ecosyst Environ* 191:99–107. <https://doi.org/10.1016/j.agee.2014.01.024>
78. Van Zwieten L, Kimber S, Morris S, Chan KY, Downie A, Rust J, Joseph S, Cowie A (2010) Effects of biochar from slow pyrolysis of papermill waste on agronomic performance and soil fertility. *Plant Soil* 327:235–246. <https://doi.org/10.1007/s11104-009-0050-x>
79. Singh B, Singh BP, Cowie AL (2010) Characterisation and evaluation of biochars for their application as a soil amendment. *Soil Res* 48:516–525. <https://doi.org/10.1071/SR10058>
80. Bolan N, Sarmah AK, Bordoloi S, Bolan S, Padhye LP, Van Zwieten L, Sooriyakumar P, Khan BA, Ahmad M, Solaiman ZM, Rinklebe J, Wang H, Singh BP, Siddique KHM (2023) Soil acidification and the liming potential of biochar. *Environ Pollut* 317:120632. <https://doi.org/10.1016/j.envpol.2022.120632>
81. Wang K, Peng N, Lu G, Dang Z (2020) Effects of pyrolysis temperature and holding time on physicochemical properties of swine-manure-derived biochar. *Waste Biomass Valori* 11:613–624. <https://doi.org/10.1007/s12649-018-0435-2>
82. Hossain MZ, Bahar MM, Sarkar B, Donne SW, Wade P, Bolan N (2021) Assessment of the fertilizer potential of biochars produced from slow pyrolysis of biosolid and animal manures. *J Anal Appl Pyrol* 155:105043. <https://doi.org/10.1016/j.jaap.2021.105043>
83. Jindo K, Mizumoto H, Sawada Y, Sanchez-Monedero MA, Sonoki T (2014) Physical and chemical characterization of biochars derived from different agricultural residues. *Biogeosciences* 11:6613–6621. <https://doi.org/10.5194/bg-11-6613-2014>
84. Chen B, Zhou D, Zhu L (2008) Transitional adsorption and partition of nonpolar and polar aromatic contaminants by biochars of pine needles with different pyrolytic temperatures. *Environ Sci Technol* 42:5137–5143. <https://doi.org/10.1021/es8002684>
85. Keiluweit M, Nico PS, Johnson MG, Kleber M (2010) Dynamic molecular structure of plant biomass-derived black carbon (biochar). *Environ Sci Technol* 44:1247–1253. <https://doi.org/10.1021/es9031419>
86. Vasseghian Y, Sezgin D, Nguyen DC, Hoang HY, Yilmaz MS (2023) A hybrid nanocomposite based on CuFe layered double hydroxide coated graphene oxide for photocatalytic degradation of trimethoprim. *Chemosphere* 322:138243. <https://doi.org/10.1016/j.chemosphere.2023.138243>
87. Ahmad M, Lee SS, Dou X, Mohan D, Sung JK, Yang JE, Ok YS (2012) Effects of pyrolysis temperature on soybean stover- and peanut shell-derived biochar properties and TCE adsorption in water. *Bioresour Technol* 118:536–544. <https://doi.org/10.1016/j.biortech.2012.05.042>
88. Allam F, Elnouby M, El-Khatib KM, El-Badan DE, Sabry SA (2020) Water hyacinth (*Eichhornia crassipes*) biochar as an alternative cathode electrocatalyst in an air-cathode single chamber microbial fuel cell. *Int J Hydrogen Energy* 45:5911–5927. <https://doi.org/10.1016/j.ijhydene.2019.09.164>
89. Chatterjee R, Sajjadi B, Chen WY, Mattern DL, Hammer N, Raman V, Dorris A (2020) Effect of pyrolysis temperature on physicochemical properties and acoustic-based amination of biochar for efficient CO<sub>2</sub> adsorption. *Front Energy Res* 8:1–18. <https://doi.org/10.3389/fenrg.2020.00085>
90. Liu X, Zhou Y, Zhou W, Li L, Huang S, Chen S (2015) Biomass-derived nitrogen self-doped porous carbon as effective metal-free catalysts for oxygen reduction reaction. *Nanoscale* 7:6136–6142. <https://doi.org/10.1039/C5NR00013K>
91. Vinayakumar K, Palliyarayil A, Prakash PS, Kumar NS, Sil S (2022) A facile one pot synthesis of biocarbon derived from water hyacinth and development of pellets for CO<sub>2</sub> capture applications. *Biomass Bioenerg* 167:106648. <https://doi.org/10.1016/j.biombioe.2022.106648>
92. Lee JW, Kidder M, Evans BR, Paik S, Buchanan Iii AC, Garten CT, Brown RC (2010) Characterization of biochars produced from cornstovers for soil amendment. *Environ Sci Technol* 44:7970–7974. <https://doi.org/10.1021/es101337x>
93. Kalderis D, Kotti MS, Méndez A, Gascó G (2014) Characterization of hydrochars produced by hydrothermal carbonization of rice husk. *Solid Earth* 5:477–483. <https://doi.org/10.5194/se-5-477-2014>
94. Yang C, Liu J, Lu S (2021) Pyrolysis temperature affects pore characteristics of rice straw and canola stalk biochars and biochar-amended soils. *Geoderma* 397:115097. <https://doi.org/10.1016/j.geoderma.2021.115097>
95. Liang B, Lehmann J, Solomon D, Kinyangi J, Grossman J, O'Neill B, Skjemstad JO, Thies J, Luizão FJ, Petersen J, Neves EG (2006) Black carbon increases cation exchange capacity in soils. *Soil Sci Soc Am J* 70:1719–1730. <https://doi.org/10.2136/sssaj2005.0383>
96. Hu Z, Ma X, Li L (2015) Optimal conditions for the catalytic and non-catalytic pyrolysis of water hyacinth. *Energy Convers Manag* 94:337–344. <https://doi.org/10.1016/j.enconman.2015.01.087>

97. Nagel K, Hoilett NO, Mottaleb MA, Meziani MJ, Wistrom J, Bellamy M (2019) Physicochemical characteristics of biochars derived from corn, hardwood, miscanthus, and horse manure biomasses. *Commun Soil Sci Plant Anal* 50:987–1002. <https://doi.org/10.1080/00103624.2019.1594881>
98. Batista E, Shultz J, Matos TTS, Fornari MR, Ferreira TM, Szpoganicz B, de Freitas RA, Mangrich AS (2018) Effect of surface and porosity of biochar on water holding capacity aiming indirectly at preservation of the Amazon biome. *Sci Rep* 8:10677. <https://doi.org/10.1038/s41598-018-28794-z>
99. Mangrich A, Cardoso E, Doumer M, Romão L, Vidal M, Rigol A, Novotny E (2015) Improving the water holding capacity of soils of Northeast Brazil by biochar augmentation. In: Ahuja S, de Andrade JB, Dionysiou DD, Hristovski KD, Loganathan BG (eds) *Water challenges and solutions on a global scale*, ACS Publications, Washington DC, pp 339–354. <https://doi.org/10.1021/bk-2015-1206.ch016A>

**Publisher's Note** Springer Nature remains neutral with regard to jurisdictional claims in published maps and institutional affiliations.

Springer Nature or its licensor (e.g. a society or other partner) holds exclusive rights to this article under a publishing agreement with the author(s) or other rightsholder(s); author self-archiving of the accepted manuscript version of this article is solely governed by the terms of such publishing agreement and applicable law.